
Contribution of Aerosol-Cloud-Vegetation Interactions to the Hydrological Cycle
during the Amazonian Biomass Burning Season

JOHN TEN HOEVE

Stanford University, Stanford, California

Department of Civil and Environmental Engineering

Mentor: Dr. Lorraine Remer

NASA Goddard Space Flight Center

Contribution of Aerosol-Cloud-Vegetation Interactions to the Hydrological Cycle during the Amazonian Biomass Burning Season

John E. Ten Hoeve, Lorraine A. Remer, Mark Z. Jacobson

Abstract

The effect of aerosols on the hydrological cycle remains one of the largest uncertainties in our climate system. Biomass burning, from both deforestation and annual agricultural burning, is the largest anthropogenic source of these aerosols in the Southern Hemisphere. Biomass burning aerosols have competing effects on clouds: Depending on the level of aerosol loading and the background cloud characteristics, aerosols can either inhibit or invigorate cloud formation and/or growth. Many observational studies have analyzed the effect of aerosols on clouds over the Amazon; however, none have conducted a detailed analysis of the varying effects of aerosols over different land surface types. This study is focused on a 3° NE x 4° WE region in Rondônia, Brazil that encompasses extensive, contiguous areas of both forested and deforested land. High resolution aerosol, cloud, water vapor, and atmospheric profile data from the Moderate Resolution Imaging Spectroradiometer (MODIS), as well as aerosol and water vapor data from the Aerosol Robotic Network (AERONET) are used collectively to examine the effect of aerosols on water vapor loading and warm cloud development over a forest and pasture during the burning season months of August through October. A perceptible difference in water vapor loading as a function of aerosol optical depth (AOD) between the forest and pasture is detected by both instruments. This difference may be attributed to enhanced photosynthetic activity caused by higher surface diffuse radiation fluxes in aerosol loaded conditions. At a certain AOD threshold, however, the reduction in total radiation reaching the surface outweighs the increase in diffuse radiation and the relationship between water vapor and AOD over forest and pasture becomes similar. The difference in water vapor over the two land surface types, in turn, has a noticeable effect on warm cloud cover, as observed by the MODIS instrument.

Introduction

A variety of observational and modeling studies have examined the effect of aerosols on the regional hydrometeorology over the Amazon Basin during the biomass burning season (Feingold et al. 2005, Kaufman et al. 1992, Kaufman et al. 1997, Koren et al. 2004, Koren et al. 2008, Martins et al. 2009, Yu et al. 2007, Zhang et al. 2008). Other studies have probed into the regional climate effects of deforestation through changes in surface energy and water vapor fluxes and land-atmosphere interactions (Correia et al. 2007, Cutrim et al. 1995, Henderson-Sellers et al. 1984, Negri et al. 2004, Nobre et al. 1991, Roy et al. 2002, Wang et al. 2009). To our knowledge, no observational study has bridged these two areas of research and studied the effect of aerosols on regional hydrometeorology over different land surface types.

The biomass burning studies show that aerosols impact clouds through both microphysical and radiative mechanisms (Kaufman et al. 2006, Koren et al. 2008, Rosenfeld et al. 2008). Depending on the concentration of aerosol, its chemical composition, size distribution, and background cloud characteristics, aerosols can either inhibit or invigorate cloud formation and/or growth. Carbonaceous biomass burning aerosols can absorb solar radiation, warming the aerosol layer and reducing the radiation reaching the surface (Koren et al. 2004). This effect cools the surface, stabilizes the lower troposphere, suppresses surface heat and moisture fluxes, and slows the hydrological cycle (Andreae et al. 2004, Jacobson et al. 2002). Evaporation of

clouds within the aerosol layer may also occur due to the increase in temperature and decrease in relative humidity caused by aerosol absorption of solar radiation (Jacobson et al. 2002). These radiative effects primarily suppress cloud formation and growth.

Microphysical effects, on the other hand, serve to enhance cloud formation and growth. Biomass burning aerosols are hygroscopic and can serve as cloud condensation nuclei (CCN) (Andreae et al. 2004). Expansion chamber experiments have shown that the addition of CCN nucleates a larger number of smaller cloud droplets, and these droplets are therefore slower to coalesce to form precipitation (Gunn et al. 1957, Squires et al. 1958). These aerosol-processed clouds are more reflective and have longer lifetimes (Twomey 1977, Albrecht 1989). More recent studies have shown that these polluted clouds may become invigorated, with higher liquid water paths and cloud top pressures (Andreae et al. 2004, Khain et al. 2005, Rosenfeld et al. 2008). The delay of raindrop formation in polluted clouds suppresses downdrafts, which allows for the generation of greater updrafts and stronger convection. The updrafts carry water vapor to higher altitudes, where additional energy from the latent heat of freezing may be released, further invigorating convection (Andreae et al. 2004, Rosenfeld et al. 2008). Increases in aerosol optical depth have also been linked to increases in cloud fraction, particularly at low AODs (Koren et al. 2005, Lin et al. 2006, Myhre et al. 2007).

Later studies have illustrated that there may be a smooth transition between these competing microphysical and radiative effects (Koren et al. 2008, Rosenfeld et al. 2008). Using MODIS Level 3 data over the Amazon, Koren et al. 2008 shows that microphysical processes dominate at lower AODs, increasing cloud fraction and height, whereas radiative processes dominate at higher AODs, decreasing cloud fraction and height. The study also shows that the relative contributions of the microphysical and radiative effects are strongly tied to the initial cloud fraction – the radiative absorption effect begins to dominate at lower values of AOD for lower initial cloud fractions. This is due to the aerosol absorption cloud fraction feedback (AFF): Stabilization of the near-surface atmosphere due to the aerosol layer initially reduces cloudiness, which then exposes greater areas under the aerosol layer to solar radiation, which then become destabilized (Koren et al. 2008). For low cloud fractions, more of the aerosol layer is available for absorption, resulting in a stronger feedback (Koren et al. 2008). For higher cloud fractions, microphysical invigoration will dominate for the same AOD value. Therefore, adding small concentrations of AOD to a sparse or dense cloud field can have entirely opposite effects on climate forcing.

Various studies have also examined the effects of deforestation on the regional hydrometeorology of the Amazon. Depending on the structure and scale of the deforestation, contrasting effects on clouds and precipitation are observed (D’Almeida et al. 2007). The majority of studies find an increase in surface temperature and a decrease in evapotranspiration over deforested regions (Gash et al. 1997, Correia et al. 2007, Salati et al. 1991, Shukla et al. 1990, Nobre et al. 1991, Wang et al. 2009). Some modeling studies predict significant decreases in precipitation associated with unrealistic large-scale deforestation; however, these studies find hydrological feedbacks that are very different than what actually occurs on local and regional scales of deforestation (Werth et al. 2002, D’Almeida et al. 2007). However, a reduction in precipitation is observed even in studies that treat deforestation at fine scales due to the high amount of precipitation recycling in the region (Franken et al. 1984, Salati et al. 1991). Evapotranspiration is reduced over the pasture during the dry season by two pathways: (1) a higher surface albedo reflects more available radiative energy back to space; and (2) the availability of soil moisture at the rooting zone is reduced. It is estimated that 50%-60% of total

rainfall in the Amazon is derived from evapotranspiration (D'Almeida et al. 2007, Marques et al. 1977, Salati et al. 1991). Other studies put the local effect of evapotranspiration lower, between 25% and 35% (Eltahir et al. 2004). In either case, changes in the land cover could have large impacts on evapotranspiration, water cycling, and cloud cover and precipitation. Regional modeling studies have estimated a reduction in evapotranspiration of about 30% over deforested regions of the Amazon (Nobre et al. 1991, Shukla et al. 1990).

Smaller scale deforestation (i.e. the observed fish bone pattern) spawns mesoscale circulations that arise from land surface heterogeneities on the finer scale (Roy et al. 2002, Segal et al., 1988, Wang et al. 1996, Wang et al. 2000, Wang et al. 2009). Enhanced shallow convection over deforested regions is caused in part by a land breeze from nearby moisture-rich forests. When this moist land breeze reaches unstable air over the deforested region (due to greater surface heating), it rises to form clouds (Segal et al. 1988, Roy et al. 2002). Several observational studies have shown an increase in shallow convection over disturbed regions of the Amazon due to this direct thermal circulation, particularly in the state of Rondônia, Brazil (Calvert et al. 1997, Cutrim et al. 1995, Negri et al. 2004).

The overlap of these two areas of study, aerosol effects on clouds and deforestation effects on clouds, is centered around the impact of aerosols on surface-atmosphere interactions, and how those impacts feed back to cloud formation. This study probes into two primary questions: (1) how does the temperature profile change with increasing aerosol optical depth over different land surface types; and (2) what is the response of vegetation to altering the amount and diffuse fractionation of radiation reaching the surface from aerosols? Modeling and observational studies have illustrated that the lower atmosphere over the Amazon increases in stability with increasing aerosol optical depth (Davidi et al. 2009, Feingold et al. 2005, Koren et al. 2004). Few observational studies, however, have probed into the varying direct and indirect effects of aerosols over different land surface types using remote sensing data (Chen et al. 2009).

A large number of studies, particularly field experiments, have analyzed the impact of aerosols on photosynthetic rates, gas and energy fluxes, and carbon uptake (i.e. net ecosystem exchange (NEE)) (Min et al. 2005, Oliveira et al. 2007, Roderick et al. 2001). These, and a variety of other studies, suggest that the increase in diffuse photosynthetically active radiation due to the addition of sparse clouds or aerosols will result in the augmentation of photosynthetic rates and net ecosystem exchange (Knobl et al. 2008, Roderick et al. 2001, Still et al. 2009). Even though additional scattering of light by aerosols results in a reduction of total photosynthetically active radiation (PAR) that reaches the surface, it has been shown that NEE will increase to a certain AOD threshold, at which the reduction in total radiation outweighs the increase in diffuse radiation and NEE decreases (Oliveira et al. 2007). The increase in diffuse radiation enhances photosynthesis and transpiration by several pathways: (1) through an increase in radiation reaching light-limited shade leaves; (2) through an increase in light-use efficiency since photosynthetic rates of leaves exposed to direct sunlight saturate at high irradiances (Roderick et al. 2001, Still et al. 2009); and (3) through lower leaf temperatures which reduce plant respiration rates (Baldocchi et al. 1997, Gu et al. 2002, Knapp et al. 1989, Rocha et al. 2004). It has been suggested that the light use efficiency of diffuse radiation is over two times greater than direct beam radiation, and the water use efficiency can be three times greater since the broader angular distribution of light is more effectively intercepted by plants (Gu et al. 2002, Min et al. 2005). Modeling studies have shown that aerosols may increase transpiration rates up to a certain AOD threshold, which is proposed, but not shown, to affect local and regional climate (Knobl et al. 2008, Steiner et al. 2005, Niyogi et al. 2007). Furthermore, in situ studies

have illustrated that change in NEE with increasing AOD is different over different landscapes, which suggests a possible difference in land-atmosphere interactions may be observed over deforested and forested land in the Amazon (Niyogi et al. 2004).

Data and Methods

MODIS is a first-of-its kind instrument in that it provides relatively high spatial resolution (250 – 500 m), while also achieving near global coverage on a daily basis (Salomonson et al. 1989). Because of its high temporal and spatial resolution, large amounts of atmospheric data may be collected for small study regions. Furthermore, the instrument has been operational on the Terra satellite since 2000 and on the Aqua satellite since 2002, allowing for the study and comparison of multiple years of data. The Aqua satellite is on a sun synchronous orbit with an overpass at approximately 1:30 PM local time, whereas the Terra satellite overpasses at approximately 10:30 AM local time. The Aqua pass is chosen over the Terra pass since warm clouds are more likely to be developed in the afternoon compared to the morning. We choose MODIS over other sensors, such as the Multi-angle Imaging Spectroradiometer (MISR), due to its high resolution and because MODIS produces a variety of cloud and atmospheric profile products, which other sensors do not (Diner et al. 1997). This paper employs MODIS Swath Level 2 aerosol, cloud, water vapor, and stability products (King et al. 2003). Aerosol optical depth from the aerosol product is calculated over land and ocean at a wavelength of 0.55 μm , with a footprint of 10 km x 10 km (Kaufman et al. 1997a, Kaufman et al. 1997b, Remer et al. 2005). Validation with ground-based AERONET observations yield an overall error of $\pm 0.05 \pm 0.2\tau_a$ over land, where τ_a is the aerosol optical depth at 0.55 μm (Chu et al. 2002).

The Level 2 cloud product contains information about cloud fraction, cloud top properties, cloud phase properties, and cloud microphysical properties, calculated using fourteen of the MODIS spectral bands (Ackerman 2002). The cloud fraction and cloud top properties are produced at 5 km x 5 km resolution, whereas the microphysical properties are produced at 1 km x 1 km resolution (Platnick et al. 2003). The cloud fraction product is calculated using the 1 km cloud mask, and is clear-sky conservative. The cloud phase retrieval is based on contrasting effects of water droplets and ice crystals on the brightness temperature in the infrared bands (Platnick et al. 2003). The cloud microphysical properties include cloud optical thickness (COT), cloud effective radius, and cloud liquid water path. Liquid water path is calculated from effective radius and COT using the equation $WP=2\rho\tau_cR_c/3$ where τ_c is cloud optical thickness, R_c is effective radius, and ρ is the density of water (King et al 1997). Cloud effective radius is bias towards cloud tops due the retrieval method used, yet relative changes of effective radii, which are studied here, are assumed to be small (Nakajima et al. 1991). The 1 km and 5 km data are averaged into 10 km x 10 km grid boxes in order to conform to the Level 2 aerosol data.

Column precipitable water vapor is derived from integrating the 101 levels at which water vapor mixing ratio is calculated in the MOD07 atmospheric profile product (Seeman et al. 2002). We do not choose to use the near-IR precipitable water product due to its limitations over dark surfaces (Gao et al. 1998). Furthermore, the infrared-derived product uses a split-window technique which is more accurate over green surfaces (Gao et al. 1998). The profile algorithms are based on thermal emissions of atmospheric gases with uniform distributions, such as oxygen and carbon dioxide (Seeman et al. 2002). The moisture profile is calculated using infrared

wavelengths between 6.5 μm and 8.7 μm , whereas the temperature profile is calculated using wavelengths at 4.5 μm , and wavelengths between 13.2 – 14.4 μm (Seeman et al. 2002). For locations with a surface pressure less than 1000 hPa, the 1000 hPa temperature was calculated using the skin temperature, surface pressure, and Poisson's Equation for potential temperature. The water vapor and profile products are also produced at 5 km resolution, but are averaged to the 10 km scale to conform to the Level 2 aerosol data, similar to the cloud data. Products requiring a clear sky, such as the MOD07 products, are able to be determined for most 10 km pixels with cloud fractions less than one.

Stratification of the MODIS atmospheric data by land cover type requires an up-to-date, high-resolution land cover classification dataset. The Land Processes Distributed Active Archive Center (LP DAAC), located at the U.S. Geological Survey (USGS) Earth Resources Observation and Science (EROS) Center, provides a combined Terra/Aqua yearly land cover product - MCD12Q1 (<http://lpdaac.usgs.gov>). This product employs MODIS BRDF-adjusted surface reflectances, land surface temperature data, enhanced vegetation index data, and terrain elevation information along with neural network classification algorithms and training data to assign land cover classifications (Strahler et al 1999). The data are resampled from 500 m x 500 m resolution to 0.1° x 0.1° resolution to approximately match the resolution of the Level 2 swath aerosol, cloud and profile data. Yearly land cover classifications are currently available for the years between 2001 and 2007.

Our 3° x 4° study region encompasses the deforested region of Ji Paraná in Rondônia, Brazil, as well as a protected forest to the east (Figure 1). Green regions represent primary forest and yellow regions represent pasture. Classifications of broad-leaf forest are assigned to the forested category, and classifications of closed shrublands, open shrublands, woody savannas, savannas, grasslands, croplands, cropland and natural vegetation mosaic, and barren or sparsely vegetated are assigned to the pasture category, according to the International Geosphere-Biosphere Programme categorization scheme (Strahler et al 1999). The percentage of pasture increases with time in our fixed study region due to ongoing deforestation. Between 2002 and 2007, roughly 5% of the land in the study region was converted from forest to pasture according to the 0.1° x 0.1° resolution data. An atypically small region is chosen for this study, compared to other studies of its type, so that meteorological differences due to spatial variation will be better removed. Even though the region is small, the high spatial resolution of the Level 2 data allows for the accumulation a sufficient data record for the analysis.

To verify the results drawn from the MODIS satellite, we use AERONET data from two stations within our study region (Holben et al. 1998). During the 2002 dry season, daily measurements of aerosol optical depth and column water vapor were made over a deforested site at Abracos Hill and over the canopy at a forested site at Jaru Reserve (locations indicated in Figure 1). AERONET aerosol optical depth is measured using a spectral radiometer. Distinct AOD values are calculated from the spectral extinction of direct beam radiation at several wavelengths between 0.340 μm and 1.020 μm . The column water vapor content is calculated using the 0.940 μm band (Holben et al. 1998).

Dry season-averaged column water vapor from the NCEP/NCAR Reanalysis dataset is used to segregate moist and dry years for which MODIS data were available in our study region, between 2002 and 2007 (Kalnay et al., 1996). In general, dry years are associated with higher seasonal aerosol optical depths due to less frequent aerosol washout and more burning. In addition, the contribution of water vapor released from vegetative processes to the total water vapor burden is more discernable in dry years. For these reasons, only dry years are retained for

this analysis. For the biomass burning months between August and October, the years 2004, 2005, and 2007 were distinctly drier than 2002, 2003 and 2006 over our study region, and so the former grouping of years is selected. The months of August through October are selected due to the combination of high aerosol loading from burning and consistent high pressure meteorological conditions present these months (Nobre et al. 1998). NCEP/NCAR Reanalysis 700 hPa wind vectors are also used to remove days for which the South Atlantic Subtropical High was not the dominant weather pattern over the region, in order to better account for artificial meteorological effects in the data. All retrievals that are not considered “useful” or were considered “bad” quality according to the Level 2 quality assurance bit data were also removed. The re-sampled 10 km atmospheric aerosol, cloud, and profile data are then sorted by land cover type for each of the three years, and subsequently agglomerated for all years for both forest and pasture.

Results

Table 1 shows average values of several cloud, aerosol, and atmospheric profile parameters detected by the MODIS satellite over our study region averaged over August-October for 2004, 2005, and 2007. Only 10 km pixels that contain warm clouds are included in the average. Two-sided Kolmogorov-Smirnov tests of the cumulative distribution functions of each parameter indicate that the distributions of the pasture and forest are not drawn from the same underlying distribution, at the 5% significance level, for all parameters listed in Table 1 (Eadie et al. 1971). Thus, all values listed in Table 1 are statistically different for the two land cover types.

Warm cloud fraction is substantially higher for the pasture compared to the forest, which agrees with previous studies (Cutrim et al. 1995, Negri et al. 2004, Wang et al. 2009). In addition, a lower average cloud top pressure is observed for the pasture, which suggests more shallow cloud development over the pasture compared to the forest. This result also agrees with previous observational and modeling studies (Chagnon et al. 2004, Correia et al. 2007, Wang et al. 2000, Wang et al. 2009). A consequence of deeper warm clouds over the forest is larger average liquid water paths. Column precipitable water vapor is also higher over the forest according to the MOD07 atmospheric product, likely due to the reduction in evapotranspiration over the pasture compared to the forest (Salati et al. 1991). Also observed over the pasture is an increase in atmospheric stability, which is defined as the temperature at 850 hPa minus the temperature at 1000 hPa. The shorter roughness length and lower specific heat of the pasture result in greater surface heating, as supported by the increase in 1000 hPa temperature in Table 1. This heating is hypothesized to help spawn shallow cumulus clouds (Negri et al. 2004). The difference in stability, roughly 3 K, is similar to those found in other studies (Correia et al. 2007, Polcher 1994). Aerosol optical depth is almost identical between the two land cover types, since aerosol concentrations are often relatively homogenous for hundreds of kilometers, particularly far away from aerosol sources (Andreae et al. 2002, Procopio et al. 2003, Smirnov 2000).

The mode of the one hundred 1 km cloud phase retrievals within each 10 km pixel is used to determine cloud phase. Warm clouds are segregated from cold and unknown-phase clouds by only retaining 10 km pixels with a modal liquid water phase. Water vapor, cloud properties, and atmospheric profile products are then binned by AOD at 0.55 μm for these warm phase clouds, with each bin representing 12.5 percentile of the AOD values. This method has been used previously in other studies so that bias is not introduced through inconsistent sampling in each

bin (Lin et al. 2006). The low and high AOD boundaries are assigned to be 0.05 and 0.8. Even though AOD values higher than 0.8 are routinely observed in this region during the biomass burning season, higher values are not incorporated to prevent aerosol misclassification as cloud (Brennan et al. 2005). In this range, cloud contamination of aerosol was also found to be insignificant (Kaufman et al. 2005). Error bars representing the standard errors of the bin average (σ/\sqrt{N}) are also included. Because the number of samples is roughly equal in each bin, the standard error is directly proportional to the standard deviation of the samples in each bin. For each plot, the average Julian Day retrieved in each bin is compared between pasture and forest, to ensure that the combined data in each bin is retrieved from the same time of the year, on average, between the two land surface types. If differences in Julian Day do exist for a bin, the difference is compared to the average change in the variable between the two days to ascertain if intraseasonal changes can account for the relationships observed in the variable versus AOD plot. In almost all of the cases, the difference in average Julian Day between forest and pasture in each bin is insignificant or produces a relatively small effect. Yet, further analysis is required to ensure that inconsistent sampling is not artificially affecting results.

Figure 2a shows warm cloud fraction binned by aerosol optical depth for all pixels where warm cloud fractions are greater than zero, for August-October of 2004, 2005, and 2007. Cloud fraction is higher over the pasture for all AOD bins, as inferred from Table 1. The increase in cloud fraction with aerosol optical depth for AODs between 0.05 and 0.5 is largely attributed to microphysical processes caused by aerosols acting as cloud condensation nuclei (Albrecht 1989, Feingold et al. 2001, Koren et al. 2008, Twomey 1977). The microphysical effect appears to be about twice as strong over the pasture than over the forest, a phenomenon which is hypothesized to be related to the difference in instability over the two land surfaces. With adequate water vapor and thermodynamic instability to produce low-level warm clouds, sufficient cloud condensation nuclei may be the limiting factor for cloud formation and growth. For a more unstable atmosphere over the pasture, addition of the same amount of biomass burning aerosol in the microphysical regime may cause greater invigoration of warm clouds compared to over the more stable forest. To illustrate the proposed effect of atmospheric stability on the microphysical effect of aerosols, only cloud fractions with collocated atmospheric stabilities between -15.5 K and -16.5 K are retained in Figure 2b. The range is wide enough to collect a large enough sample size for analysis, small enough to restrict the stability values sufficiently, and is between the forest and pasture averages noted in Table 1. A similar trend in cloud fraction with AOD in the microphysical regime is now observed for both pasture and forest in Figure 2b, which suggests that increased instability over the pasture enhances the microphysical effect of aerosols on clouds. The absorption effect is not strong in either the forest or pasture because we have stratified by relatively high stabilities. If more unstable retrievals were used, the absorption effect becomes more visible (not shown).

Figure 2a also illustrates that the absorption effect over the pasture is stronger than over the forest. Between an AOD of 0.5 and 0.8, in the absorption regime, cloud fraction decreases about twice as much over the pasture AOD compared to the forest due to the semi-direct effect (Feingold et al. 2005, Koren et al. 2004, Koren et al. 2008). This effect is better explained by retaining only low cloud fractions, so that a sufficient portion of the absorbent aerosol layer is not obscured by clouds. Sparse cloud fields will be dominated by aerosol absorption, and consequently the inhibition of cloud growth, whereas more dense cloud fields will be dominated by aerosol microphysics according to the aerosol absorption cloud fraction feedback (Koren et al. 2008).

Figure 3a shows cloud fraction binned by aerosol optical depth for non-zero cloud fractions less than 0.5. The microphysical portion of the curve now only extends to AODs between 0.3 and 0.4 because more of the aerosol layer is exposed in scenes with low cloud fractions (Koren et al. 2008). Similar to Figure 2, the microphysical mechanisms are invigorated over the pasture compared to the forest due to the relative difference in atmospheric stability over the two land cover types. Yet, the absorption profile of the curve is different between the forest and pasture. The relationship between cloud fraction and AOD over the forest is relatively flat between AODs of 0.3 and 0.55, whereas cloud fraction decreases rather steadily between AODs of 0.3 and 0.8 for the pasture. One possible cause could be differences in the radiative balance of the atmosphere due to dissimilar surface albedos over the pasture and forest. Figure 3b shows the relationship between atmospheric stability and AOD for similarly stratified cloud fractions to Figure 3a. While the atmosphere over the forest is substantially more stable than the pasture, as shown in Table 1, the response of stability to increasing AOD is relatively similar between the forest and pasture, especially where differences in cloud fraction are observed between AODs of 0.3 and 0.55. Increases in stability at low AODs below 0.4 are likely due to cloud shading, and decreases in stability at high AODs are due to the increased radiation absorbed at the surface when clouds are evaporated from the semi-direct effect (Davidi et al. 2009). The minor difference in stability with increasing AOD between the forest and pasture indicates that changes in the temperature profile are not the primary cause of the effect observed in Figure 3a. Furthermore, if thermodynamic effects were the cause of the difference in Figure 3a, the absorption effect would continue to be dissimilar between forest and pasture for AODs above 0.55. The relationship between precipitable water vapor and AOD, however, does exhibit considerable differences between forest and pasture (Figure 3c). The response of water vapor to increasing AOD remains flat between AODs of 0.25 and 0.55 over the forest, along the same range that cloud fraction versus AOD remains flat in Figure 3a. The precipitable water over the pasture, however, decreases with increasing AOD above an AOD of 0.3.

The difference in the precipitable water correlation with increasing AOD between pasture and forest for AODs between 0.3 and 0.55 may be attributed to photosynthesis. We suggest that transpiration resulting from augmented photosynthesis below an AOD of 0.55 causes the higher water vapor loading observed over the forest compared to the pasture. Recall that Figure 3 includes cloud fractions above zero and less than 0.5. Scattering from both aerosols and clouds contribute to the increase in diffuse radiation at the surface in this figure. The increase in water vapor released from the forest feeds back to clouds in Figure 3a, reducing the absorption effect over the forest compared to over the pasture. Several studies have postulated the effect of these land-atmosphere aerosol interactions on regional hydrometeorology through regional modeling or in-situ field experiments, showing increases in precipitation or cloud cover with higher diffuse fractionation, but none have shown this effect on the scale of 100s of kilometers using remote sensing data (Knohl 2008, Niyogi et al. 2007, Steiner et al. 2005).

For both pasture and forest, precipitable water should decrease with increasing AOD due to reduced surface evapotranspiration from the semi-direct effect (Jacobson 2002, Koren et al. 2004, Koren et al. 2008). The increase in precipitable water with AOD between AODs of 0.05 and 0.3 is an apparent aerosol effect derived from the correlation of AOD with precipitable water early in the biomass burning season. Precipitable water increases consistently between August and October as the winter dry season transitions to the summer wet season (Nobre et al. 1998). During the first two weeks of August, average aerosol optical depth also increases rapidly as the biomass burning season ramps up (Figure 4). At the conclusion of the season, AOD decreases

rapidly as biomass burning slows, although not as dramatically as the increase at the beginning of the season. Thus, at the beginning of the season precipitable water and AOD are directly correlated and at the end of the season precipitable water and AOD are indirectly correlated. To ensure that these correlations are accounted for, the first 15 days of August and last 15 days of October are removed. Removal of more than one month of data would leave us with too few data points to perform correlations. As noted earlier, the average Julian day for all data in each bin is compared between forest and pasture to ensure that intraseasonal changes in meteorological variables do not affect the comparison between the two land surface types.

Figure 5 includes the same data as Figure 3, but only including days between August 15th and October 15th. Because very few low AOD values exist during these two months, the microphysical effect is not easily observed, especially for cloud fractions less than 0.5 where the transition region is at a relatively low AOD. Reproducing Figure 5a for all cloud fractions shows the microphysical effect is still present over the same AOD interval as in Figure 2, confirming that the microphysical effect is not merely an artifact of the water vapor-aerosol-Julian Day correlation early in the season (not shown). We are confident that most of the spurious correlations are removed in Figure 5a since precipitable water no longer increases with AOD below an AOD of 0.3. Again, a difference in relationship between precipitable water and AOD is observed for the forest and pasture for AODs between 0.3 and 0.6 in Figure 5c, and again the difference in water vapor appears to have an effect on warm clouds (Figure 5a). Over the pasture, the aerosol absorption effect is much stronger than over the forest, similar to Figure 3a, particularly between AODs of 0.3 and 0.6. The relationship between stability and AOD for forest and pasture, shown in Figure 5b, again suggests that thermodynamic mechanisms are likely to not be the cause of the differences exhibited in Figure 5a. The trend in stability with AOD is not markedly different between forest and pasture.

To further support that enhancement of photosynthesis is the cause of the difference in column water vapor between forest and pasture, similar plots to Figure 3 are constructed, but for cloud fractions greater than 0.5. Figure 6a shows the relationship between cloud fraction and AOD for these high cloud fractions. Unlike Figure 3a, where forest and pasture presented different responses of cloud fraction to increasing AOD, Figure 6a shows a similar relationship between forest and pasture throughout the range of AODs. The change in cloud fraction with AOD has a nearly identical magnitude in both the microphysical and radiative regimes, as expected. High cloud fractions reduce the scattering effect of both aerosols and clouds because a high fraction of incoming solar radiation is reflected by the cloud tops instead of being scattered by aerosols or the sides of clouds. As a result, the difference in precipitable water with AOD along the range of AODs is small between forest and pasture (Figure 6b), particularly when compared to Figure 3c. The small difference in precipitable water in Figure 6b results in a relationship between cloud fraction and AOD that is similar between forest and pasture in Figure 6a. The transition region between microphysical and radiative processes occurs at a higher AOD than in Figure 3a, in accordance with the aerosol absorption cloud fraction feedback (Koren et al. 2008). Figure 6c is similar to Figure 6b, but stratified for days between August 15th and October 15th. Change in precipitable water vapor with AOD is again similar for forest and pasture, supporting the hypothesis that differences in photosynthetic rates between forest and pasture result in the observed changes in precipitable water.

We also employ AERONET data to verify results obtained from the MODIS satellite. Figure 1 shows the location of the two AERONET stations used in the study. The Jaru Reserve forest site was operated only for the biomass burning season of 2002, so only one year of data is

available for comparison with the Abracos Hill pasture site. However, due to the high temporal resolution of the AERONET data, it is possible to stratify the data even further than the satellite data while still retaining a large enough sample size for analysis. A shorter time period ensures that correlations of aerosol optical depth and precipitable water with Julian Day are not present in the data. Because AERONET data are conservatively cloud-screened, any differences in precipitable water with AOD between forest and pasture may be solely attributed to the effect of aerosols (Holben et al. 1998, Smirnov et al. 2000). Figure 7a depicts precipitable water binned by AOD for August 15th-October 25th, 2002. Differences between forest and pasture are present for AODs between 0.3 and 0.6, similar to the observations of the MODIS satellite which used completely different years but the same days within the biomass burning season. Figure 7b is similar to Figure 7a, but it contains even further stratified data to only days in the month of September. Again, a difference between forest and pasture is observed between 0.3 and 0.6. Missing data at low aerosol optical depths for the Abracos Hill site is due to the lack of low aerosol loading days during the height of the biomass burning season in September.

The hypothesis that photosynthesis is the driver behind the differences in the trends of precipitable water versus AOD between pasture and forest is supported by both satellite and ground-based measurements. As stated in the Introduction, various studies have analyzed the response of net ecosystem exchange to aerosol loading of the Amazon, and have found that photosynthesis is enhanced due to increases in the proportion of diffuse radiation, but is then inhibited when the reduction in total radiation becomes too great. Over the Jaru Forest Reserve, Oliveira et al. 2007 finds that the switch from enhancement to inhibition of NEE occurs at a relative irradiance of approximately 0.6 (defined as the total downward radiation with clouds and aerosols divided by the total downward radiation in a cloudless, clean sky), which corresponds to an aerosol loading of approximately 1.6 at 0.5 μm . Our results show that aerosols may enhance photosynthesis up to an aerosol optical depth of about 0.6, which corresponds to a relative irradiance of about 0.9. Our analysis underpredicts the range at which diffuse radiation will enhance photosynthesis, compared to Oliveira et al. 2007, however our study analyzes evapotranspiration while their study analyzes CO₂ fluxes.

Other studies show increased water use efficiency and transpiration with higher diffuse fractionation of light, which logically translates into greater surface latent heat fluxes and higher precipitable water contents (Knohl et al. 2008, Min et al. 2005). Modeling results from Knohl et al. 2008 show increases in transpiration between diffuse fractions of 0 and 0.4 for a deciduous temperate forest in central Germany. Another study that characterized the diffuse fraction of radiation as a function of AOD over the Amazon suggests that the diffuse fraction is roughly 0.4 for cloud-free aerosol optical depths of about 0.6 (Yamasoe et al. 2008). If transpiration responds similarly to increased diffuse fractionation over broadleaf evergreen forests as deciduous temperate forests in Knohl et al. 2008, it would support our hypothesis that diffuse fractionation of sunlight below an AOD of 0.6 increases photosynthesis, transpiration, and column water vapor.

This study follows a method similar to previous studies that have analyzed aerosol-cloud interactions (Koren et al. 2008, Yu et al. 2007). The aerosol-cloud-vegetation relationships that have been discovered are believed to be authentic because many preventative steps were taken to remove spurious correlations and contamination of the results. Yu et al. describes the motivation behind many of the steps taken here and in these previous studies (Yu et al. 2007). In addition, because this study primarily focuses on *differences* in aerosol effects on clouds between two nearby locations, influence of atmospheric processes that can cause bias in the absolute results

(i.e. 3-D cloud effect, aerosol humidification effect, meteorology effect) will likely not play a significant role (Kaufman et al. 2005, Koren et al. 2005, Wen et al. 2006). Differences between this study and in-situ experiments may be attributed to the differences in sampling techniques between the two studies. Furthermore, the ground-based measurements, including AERONET, include samples from multiple times of the day and multiple solar zenith angles, while the satellite only takes one measurement per day at a relatively constant solar zenith angle for each location throughout the season.

Conclusions

This study finds differences in the aerosol effect on warm clouds over forested and deforested regions in a small area of Rondônia, Brazil. The transition regime between microphysical and radiative effects changes with initial cloud fraction for both land surface types, which we expect from the aerosol absorption cloud fraction feedback (Koren et al. 2008). The microphysical regime forcing is shown to be greater over the pasture compared to the forest due to the relative instabilities over the two land cover types. Stratification of the data by stability confirms this hypothesis. For low cloud fractions in particular, we find that the aerosol effect on warm clouds over pastures and forests are different, especially in the absorption regime. It is suggested that water vapor released from the forest due to enhanced photosynthetic rates in aerosol loaded conditions feeds back to clouds, competing with the absorption effect over the forest compared to the pasture. Results are compared to previous studies that have explored responses in water vapor and carbon fluxes to changes in the diffuse radiation fraction due to aerosols. Our study shows good agreement with these previous studies, specifically for those studies that have specifically analyzed the response of transpiration with AOD.

Analysis of cloud fraction versus AOD for high cloud fractions shows a similar trend in cloud fraction with AOD for both the forest and pasture. The similarity is attributed to lack of exposed aerosols (and sparse cloud fields) which prevents the diffuse fractionation of sunlight. Because the diffuse fraction is less, the forest does not respond with enhanced photosynthesis, and the aerosol effects on warm clouds are similar. The transition from the microphysical to radiative regimes occurs at a higher AOD, due to the aerosol absorption cloud fraction feedback. This study should be followed by detailed model simulations as well as additional field campaigns that study the change in energy and latent heat fluxes over forested and deforested regions in the Amazon for varying levels of AOD. Detailed 3D canopy models that take into consideration responses of photosynthesis to the diffuse fractionation of light, coupled with an atmospheric model to treat land-atmosphere feedbacks, is required to confirm the hypotheses suggested here (Knohl et al. 2008).

References

- Ackerman, S. A., Strabala, K. I., Menzel, W. P., Frey, R. A., Moeller, C. C., and Gumley, L. E.: Discriminating clear sky from clouds with MODIS, *J. Geophys. Res.*, 103(D24), 32,141 - 32,157, 2002.
- Albrecht, B. A., Aerosols, cloud microphysics, and fractional cloudiness, *Science*, 245, 1227-1230, 1989.
- Andreae, M. O., Artaxo, P., Brandão, C., Carswell, C., Ciccioli, P., et al.: Biogeochemical cycling of carbon, water, energy, trace gases, and aerosols in Amazonia: The LBA-EUSTACH experiments, *J. Geophys. Res.*, 107(D20), 8066-8091, 2002.
- Andreae, M.O., Rosenfeld, D., Artaxo, P., Costa, A. A., Frank, G. P., Longo, K. M., and Silva-Dias, M. A. F.: Smoking rain clouds over the Amazon, *Science*, 303, 1337 – 1342, 2004.
- Baldocchi, D. D., Vogel, C. A., and Hall, B.: Seasonal variation of carbon dioxide exchange rates above and below a boreal jackpine forest, *Agric. For. Meteorol.*, 83, 147-170, 1997.
- Brennan, J. I., Kaufman, Y. J., Koren, I., and Li, R.: Aerosol-cloud interaction – misclassification of MODIS clouds in heavy aerosol, *IEEE Transaction, Geoscience and Remote Sensing*, 43(4), 911-915, 2005.
- Calvert, J. –C., Santos-Alvala, R., Jaubert, G., Delire, C., Nobre, C., Wright, I., and Noilhan, J.: Mapping surface parameters for mesoscale modeling in forested and deforested southwestern Amazonia, *Bull. Amer. Meteor. Soc.*, 78, 413-423.
- Chagnon, F. J. F., Bras, R. L. and Wang, J. Climatic shift in patterns of shallow clouds over the Amazon, *Geophys. Res. Lett.*, 31(L24212), 2004.
- Chen, Y., Li, Q., Kah, R. A., Randerson, J. T., and Diner, D. J.: Quantifying aerosol direct radiative effect with Multiangle Imager Spectroradiometer observations: top-of-atmosphere albedo change by aerosols based on land surface types, *J. Geophys. Res.*, 114, 2009.
- Chu, D. A., Kaufman, Y. J., Ichoku, C., Remer, L. A., Tanré, D., and Holben, B. N.: Validation of MODIS aerosol optical depth retrieval over land, *Geophys. Res. Lett.*, 29(12), 2002.
- Correia, F. W. S., Alvala, R. C. S., and Manzi, A. O.: Modeling the impacts of land cover change in Amazonia: a regional climate model (RCM) simulation study, *Theoretical and Applied Climatology*, 93, 225-244, 2007.
- Cutrim, E., D., Marin, W., and Rabin, R.: Enhancement of cumulus clouds over deforested lands in Amazonia. *Bull. Amer. Meteor. Soc.*, 76, 1801-1805, 1995.
- D’Almeida, C. D., C. J. Vorosmarty, Hurr, G. C., Marengo, J. A., Dingman, S. L., and Keim, B. D.: The effects of deforestation on the hydrological cycle in Amazonia: a review on scale and resolution, *Int. J. Clim.*, 27, 633-647, 2007.
- Davidi, A., Koren, I., and Remer, L.: Direct measurements of the effect of biomass burning over the Amazon on the atmospheric temperature profile. *Atmos. Chem. Phys. Discuss*, 9, 12007-12025, 2009, in review.
- Diner, D. J., Beckert, J. C., Heilly, T. H., Bruegge, C. J., Conel, J. E., Kahn, R. A., and Martonchik, J. V., Multi-angle Imager Spectroradiometer (MISR) instrument description and experiment overview, *IEEE Trans. On Geosci. And Rem. Sens.*, 1997.

- Eadie, W.T., Drijard, D., James, F.E., Roos, M., and Sadoulet, B.: *Statistical Methods in Experimental Physics*. Amsterdam: North-Holland, 269–271, 1971.
- Feingold, G., Remer, L. A., Ramaprasad, J., and Kaufman, Y.: Analysis of smoke impacts on clouds in Brazilian biomass burning regions: an extension of Twomey's approach, *J. Geophys. Res.*, 106, 22907-22922, 2001.
- Feingold, G., Jiang, H, and Harrington, J. Y.: On smoke suppression of clouds in Amazonia, *Geophys. Res. Lett.*, 32(L02840), 2005.
- Gao, B.-C., and Kaufman, Y. J.,: The MODIS Near-IR Water Vapor Algorithm – Algorithm Theoretical Basis Document, NASA Goddard Space Flight Center., 1998.
- Gash, J. H. C., and Nobre, C. A.: Climatic effects of Amazonian deforestation: some results from ABRACOS., *Bull. Amer. Meteor. Soc.*, 78, 823-830.
- Gu, L., Baldocchi, D., Verma, S. B., Black, T. A., Vesala, T., Falge, E. M., and Dowty, P. R.: Advantages of diffuse radiation for terrestrial ecosystem productivity, *J Geophys. Res.*, 107(D6), 2002.
- Gunn, R. and Phillips, B. B.: An experimental investigation of the effect of air pollution on the initiation of rain, *J. Meteorol.*, 14, 272-280, 1957.
- Henderson-Sellers, A., and Gornitz, V.: Possible climatic impacts of land cover transformation with particular emphasis on tropical deforestation, *Climatic Change*, 6, 231-258, 1984.
- Holben B.N., Eck, T.F., Slutsker, I., Tanré, D., Buis, J. P., Setzer, A., Vermote, E., Reagan, J. A., Kaufman, Y. J., Nakajima, T., Lavenu, F., Jankowiak, I., and Smirnov, A.,: AERONET - A federated instrument network and data archive for aerosol characterization, *Rem. Sens. Environ.*, 66, 1-16, 1998.
- Jacobson, Mark. Z.: Control of fossil-fuel particulate black carbon and organic matter, possibly the most effective method of slowing global warming. *J. Geophys. Res.*, 107(D19), 2002.
- Kalnay, E., Kanamitsu, M., R., Kistler, W., et al.: The NCEP/NCAR 40-Year Reanalysis Project. *Bulletin of the American Meteorological Society*, 77, 437-470, 1996.
- Kaufman, Y. J., and Fraser, R. S.: The effect of smoke particles on clouds and climate forcing, *Science*, 277, 1636 – 1639, 1997.
- Kaufman, Y. J., and Nakajima, T.: Effect of Amazon smoke on cloud microphysics and albedo – analysis from satellite imagery, *J. App. Met.*, 32, 729-744, 1992.
- Kaufman, Y. J., Koren, I., Remer, L. A., Rosenfeld, D., and Rudich, Y.: The effect of smoke, dust, and pollution aerosol on shallow cloud development over the Atlantic Ocean, *Proc. Nat. Acad. Sci.*, 102, 11207, 2005.
- Kaufman, Y. J., Remer, L. A., Tanré, D., Li, R. –R., Kleidman, R., Matoo, S., et al.: A critical examination of the residual cloud contamination and iurnal sampling effects on MODIS estimates of aerosol over ocean, *IEEE Trans. on Geos. and Rem. Sens*, 43(12), 2886-2897, 2005.
- Kaufman, Y. J., Tanré, D., Gordon, H. R., Nakajima, T., Lenoble, J., Frouin, R., Grassl, H., Herman, B. M., King, M. D., and Teillet, P. M.: Passive remote sensing of tropospheric aerosol and atmospheric correction for the aerosol effect, *J. Geophys. Res.*, 102, 16,815-16,830, 1997a.
- Kaufman, Y. J., Tanré, D., Remer, L. A., Vermote, E. F., Chu, A., and Holben, B. N.: Operational remote sensing of tropospheric aerosol over the land from EOS-MODIS, *J. Geophys. Res.*, 102, 17,051-17,068, 1997b.

- Khain, A. P., Rosenfeld, D., and Pokrovsky, A.: Aerosol impact on the dynamics and microphysics of deep convective clouds, *Q. J. R. Meteor. Soc.*, 131, 2639-2663, 2005.
- King, M. D., Menzel, W.P., Kaufma, Y.J., Tanré, D., Gao, B.-C., Platnick, S., et al.: Cloud and aerosol properties, precipitable water, and profiles of temperature and humidity from MODIS, *IEEE Trans. Geosci. Remote Sens.*, 41, 442-458, 2003.
- King, M. D., et al.: Cloud retrieval algorithms for MODIS: Optical thickness, effective particle radius, and thermodynamic phase, 79 pp., NASA Goddard Space Flight Center., Greenbelt, MD, 1997.
- Knapp, A. K., Smith, W. K., and Young, D. R.: Importance of intermittent shade to the ecophysiology of subalpine herbs. *Funct. Ecol*, 3, 753-758, 1989.
- Knohl, A. and Baldocchi, D. D.: Effects of diffuse radiation on canopy gas exchange processes in a forest ecosystem, *J. Geophys. Res.*, 113(G02023), 2008.
- Koren, I., Kaufman, Y. J., Remer, L. A., and Martins, J. V.: Measurement of the effect of Amazon smoke on inhibition of cloud formation, *Science*, 303, 1342-1345, 2004.
- Koren, I., Kaufman, Y. J., Rosenfeld, D., Remer, L. A., and Rudich, Y.: Aerosol invigoration and restructuring of Atlantic convective clouds, *Geophys. Res. Lett.*, 32, 2005.
- Koren, I., Martins, J. V., Remer, L. A., and Afargan, H.: Smoke invigoration versus inhibition of clouds over the Amazon, *Science*, 321, 946-949, 2008.
- Lin, J. C., Matsui, T., Pielke Sr., R. A., and Kummerow, C.: Effects of biomass-burning-derived aerosols on precipitation and clouds in the Amazon Basin: a satellite-based empirical study, *J. Geophys. Res.*, 111(D19204), 2006.
- Marques, J., dos Santos, J.M., Villa Nova, N.A. and Salati, E.: Precipitable water and water vapor flux between Belém and Manaus. *Acta Amazon.*, 7, 355-362, 1977.
- Martins, J. A., Silva Dias, M. A. F., and Gonçalves, F. L. T.: Impact of biomass burning aerosols on precipitation in the Amazon: a modeling case study, *J. Geophys. Res.*, 114, 2009.
- Min, et al.: 2005.: Impact of aerosols and clouds on forest-atmosphere carbon exchange, *J. Geophys. Res.*, 110(D06), 2005.
- Myhre, G., Stordal, F., Johnsrud, J., Kaufman, Y. J., Rosenfeld, D., Storelvmo, T., Kristjansson, J. E., Berntsen, T. K., Myhre, A., and Isaksen, I. S. A.: Aerosol-cloud interaction inferred from MODIS satellite data and global aerosol models, *Atmos. Chem. and Phys.*, 7, 3081-3101, 2007.
- Nakajima, T., King, M. D., Spinhirne, J. D., and Radke, R. F.: Determination of the optical thickness and effective particle radius of clouds from reflected solar radiation measurements, part II: marine stratocumulus observations. *J. Atmos. Sci.*, 48, 728-750, 1991.
- Negri, A. J., and Adler, R. F.: The impact of Amazonian deforestation on dry season rainfall, *J. Climate*, 17, 2004.
- Niyogi, D., Chang, H. -I., Chen, F., Gu, L., Kumar, A., Menon, S., and Pielke Sr., R. A.,: Potential impacts of aerosol-land-atmosphere interactions on the Indian monsoonal rainfall characteristics, *Nat. Hazards*, 42(2), 2007.
- Niyogi, D., Chang, H. -I., Saxena, V. K., Holt, T., Alapaty, K., Booker, F., Chen, F., Davis, K. J., Holben, B., Matsui, T., Meyers, T., Oechel, W. C., Pielke Sr., R. A., Wells, R., Wilson, K., and Xue, Y.: Direct observations of the effects of aerosol loading on net ecosystem CO₂ exchanges over different landscapes, *Geophys. Res. Lett.*, 31, 2004.

- Nobre, C. A., Mattos, L. F., Dereczynski, C. P., et al.: Overview of atmospheric conditions during the Smoke, Clouds and Radiation-Brazil (SCAR-B) field experiment, *J. Geophys. Res.*, 103, 31809-31820, 1998.
- Nobre, C. A., Sellers, P. J., and Shukla, J.: Amazonian deforestation and regional climate change, *J. Climate*, 4, 957-988, 1991.
- Oliveira, P. H. F., Artaxo, P., Pires, C., De Lucca, S., Procopio, A., Holben, B., Schafer, J., Cardoso, L. F., Wofsy, S. C., and Rocha, H. R.: The effects of biomass burning aerosols and clouds on the CO₂ flux in Amazonia, *Tellus*, 59B, 338-349, 2007.
- Platnick, S., King, M. D., Ackerman, S. A., Menzel, W. P., Baum, B. A., and Riedi, J. C.: The MODIS cloud products: Algorithms and examples from Terra, *IEEE Trans. Geosci. Remote Sens.*, 41(2), 459-473, 2003.
- Polcher, J., and Laval, K.: The impact of African and Amazonian deforestation on tropical climate, *J. Hydrology (Amsterdam)*, 155, 389-405, 1994.
- Procopio, A. S., Remer, L. A., Artaxo, P., Kaufman, Y. J., and Holben, B. N.: 2003: Modeled spectral optical properties for smoke aerosols in Amazonia, *Geophys. Res. Lett.*, 30(24), 2265-2270, 2003.
- Remer, L. A., Kaufman, Y. J., Tanré, D., Matoo, S., Chu, D. A., and Martins, J.V.: The MODIS aerosol algorithm, products and validation, *J. Atmos. Sci.*, 62, 947-973, 2005.
- Rosenfeld, D., Lohmann, U., Raga, G. B., O'Dowd, C. D., Kulmala, M., Fuzzi, S., Reissell, A., and Andreae, M. O.: Flood or drought: how do aerosols affect precipitation?, *Science*, 321, 1309-1313, 2008.
- Rocha, A. V., Su, H. -B., Vogel, C. S., Schmid, H. P., and Curtis, P. S.: Photosynthetic and water use efficiency responses to diffuse radiation by an aspen-dominated northern hardwood forest, *For. Sci.*, 50(6), 2004.
- Roderick, M. L., Farquhar, G. D., Berry, S. L., Noble, I. R., On the direct effect of clouds and atmospheric particles on the productivity and structure of vegetation, *Oecologia*, 129, 21-30, 2001.
- Roy, S. B., and R. Avissar.: Impact of land use/land cover change on regional hydrometeorology in Amazonia, *J. Geophys. Res.*, 107, 2002.
- Salati, E., and Nobre, C. A.: Possible climatic impacts of tropical deforestation, *Climatic Change*, 19, 1991.
- Salomonson, V. V., Barnes, W. L., Maymon, P. W., Montgomery, H. E., and Ostrow, H.: MODIS: Advanced facility instrument for studies of the Earth as a system, *IEE Trans. Geosci. Rem. Sens.*, 27, 145-153, 1989.
- Seemann, S., Borbas, E. E., Li, J., Menzel, P., and Gumley, L. E.: MODIS atmospheric profile retrieval – Algorithm Theoretical Basis Document, Cooperative Institute for Meteorological Satellite Studies, University of Wisconsin, 2006.
- Segal, M., Avissar, R., Mccumber, M. C., and Pielke, R. A.: Evaluation of vegetation effects on the generation and modification of mesoscale circulations, *J. Atmos. Sci.*, 45, 2268-2292, 1988.
- Shukla, J., Nobre, C., and Sellers, P.: Amazon deforestation and climate change, *Science*, 247, 1322 – 1325, 1990.
- Smirnov, A., Holben, B. N., Eck, T. F., Dubovik, O., and Slutsker, I.: Cloud-screening and quality control algorithms for the AERONET database, *Remote Sens. of Env.*, 73(3), 337-349, 2000.
- Squires, P., The microstructure and colloidal stability of warm clouds, *Tellus*, 10, 256-271, 1958.
- Steiner, A., and Chameides, W. L.: Aerosol induced thermal effects increase modeled terrestrial photosynthesis and transpiration, *Tellus*, 27B, 404-411, 2005.

- Still, C. J., Riley, W. J., Biraud, S. C., Noone, D. C., Buening, N. H., Randerson, J. T., Tom, M. S., Welker, J., White, J. W. C., Vachon, R., Farquhar, G. D., and Berry, J. A.: Influence of clouds and diffuse radiation on ecosystem-atmosphere CO₂ and CO¹⁸O exchanges, *J. Geophys. Res.*, 114, 2009.
- Strahler, A., Muchoney, D., Borak, J., Friedl, M., Gopal, S., Lambin, E., and Moody, A., MODIS land cover and land-cover change – Algorithm Theoretical Basis Document, Department of Geography, Boston University, 1999.
- Twomey, S., The influence of pollution on the shortwave albedo of clouds, *J. Atmos. Sci.*, 34, 1149-1152, 1977.
- Yu, H., Fu, R., Dickinson, R. E., Zhang, Y., Chen, M., and Wang, H.: Interannual variability of smoke and warm cloud relationships in the Amazon as inferred from MODIS retrievals, *Rem. Sens. Environ.*, 111, 435-439, 2007
- Wang, J., Bras, R. L., Eltahir, E. A. B.: A stochastic linear theory of mesoscale circulation induced by the thermal heterogeneity of the land surface. *J. Atmos. Sci.*, 53, 3349-3366, 1996.
- Wang, J., Bras, R. L., Eltahir, E. A. B.: The impact of observed deforestation on the mesoscale distribution of rainfall and clouds in Amazonia. *J. Hydrometeorol.*, 1, 267-286, 2000.
- Wang, J., Chagnon, F. J. F., Williams, E. R., Betts, A. K., Renno, N. O., Machado, L. A. T., Bisht, G., Knox, R., and Bras, R. L.: Impact of Deforestation in the Amazon Basin on Cloud Climatology, *PNAS*, 0810156106, 2009.
- Wen, G., Marshak, A., & Cahalan, R. F.: Impact of 3D clouds on clear sky reflectance and aerosol retrieval in a biomass burning region of Brazil, *IEEE Geosci. And Rem. Sens. Lett.*, 3, 169-172, 2006.
- Werth, D., and Avissar, R.: The local and global effects of Amazon deforestation, *J. Geophys. Res.*, 107, 2002.
- Yamasoe, M. A., and Rosário, N. E.: Changes in solar radiation partitioning reaching the surface due to biomass burning aerosol particles in the Amazon Basin, *Current Problems in Atmospheric Radiation*, 2008.
- Zhang, Y., Fu, R., Yu, H., Dickinson, R. E., Juarez, R. N., Chin, M., and Wang, H.: A regional climate model study of how biomass burning aerosol impacts land-atmosphere interactions over the Amazon, *J. Geophys. Res.*, 113, 2008.

Tables

	Forested	Deforested
Cloud Effective Radius (um)	16.8	15.6
Cloud Optical Thickness (-)	9.42	8.62
Cloud Fraction (-)	0.44	0.54
Cloud Top Pressure (hPa)	721.1	748.7
Cloud Water Path (g/m ²)	88.4	76.9
Precipitable Water Vapor (cm)	4.33	4.09
850 hPa Temperature (K)	292.2	292.8
1000 hPa Temperature (K)	307.0	310.6
T850 – T1000 (K)	-14.7	-17.9
AOD at 550 nm (-)	1.07	1.09

Table 1: Average cloud, aerosol, and atmospheric profile statistics for all warm cloud retrievals for both forested and deforested land surfaces in our study region. The averaging period is for August – October for the years 2004, 2005, and 2007.

Figures

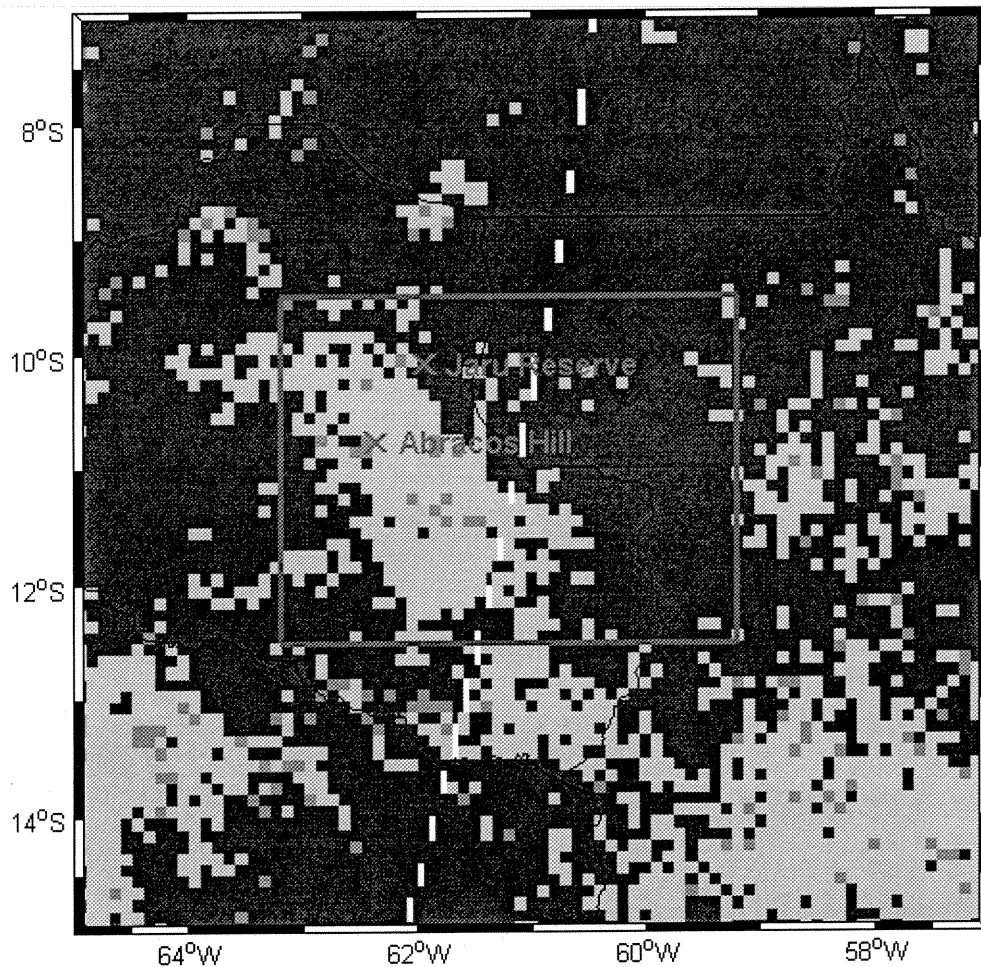


Figure 1: Land cover classifications for the year 2002. Green represents forests and yellow represents pasture or deforested land. The study region is outlined by a red box. Locations of the two AERONET stations also used in the study are marked with pink crosses.

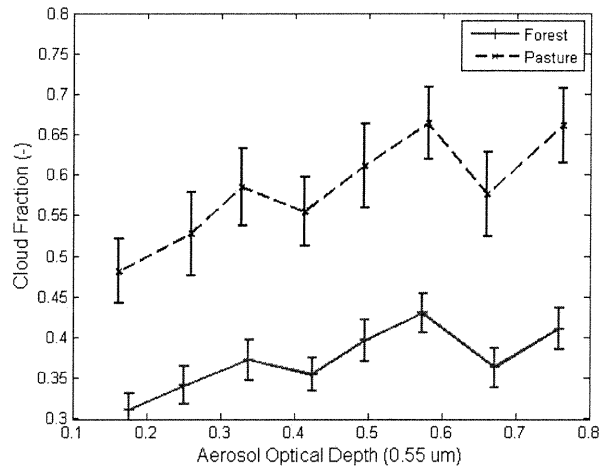
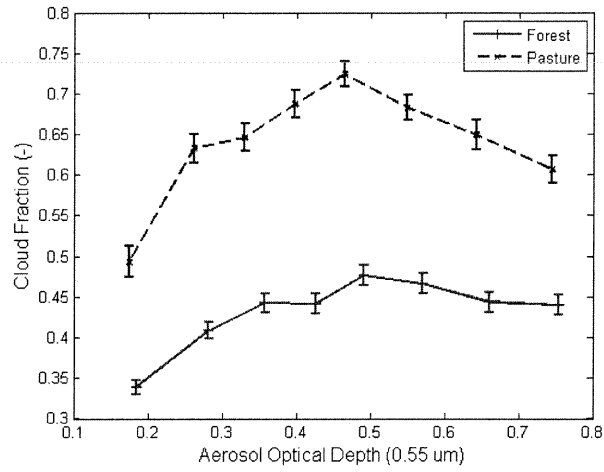


Figure 2(a): Cloud fraction binned by aerosol optical depth for all warm cloud retrievals for the months of August to October, for the years 2004, 2005, and 2007. **(b)** Same as Figure 2a but only for atmospheric stabilities between -15.5 K and -16.5 K, where stability is defined as the difference in temperature at 850 hPa and 1000 hPa.

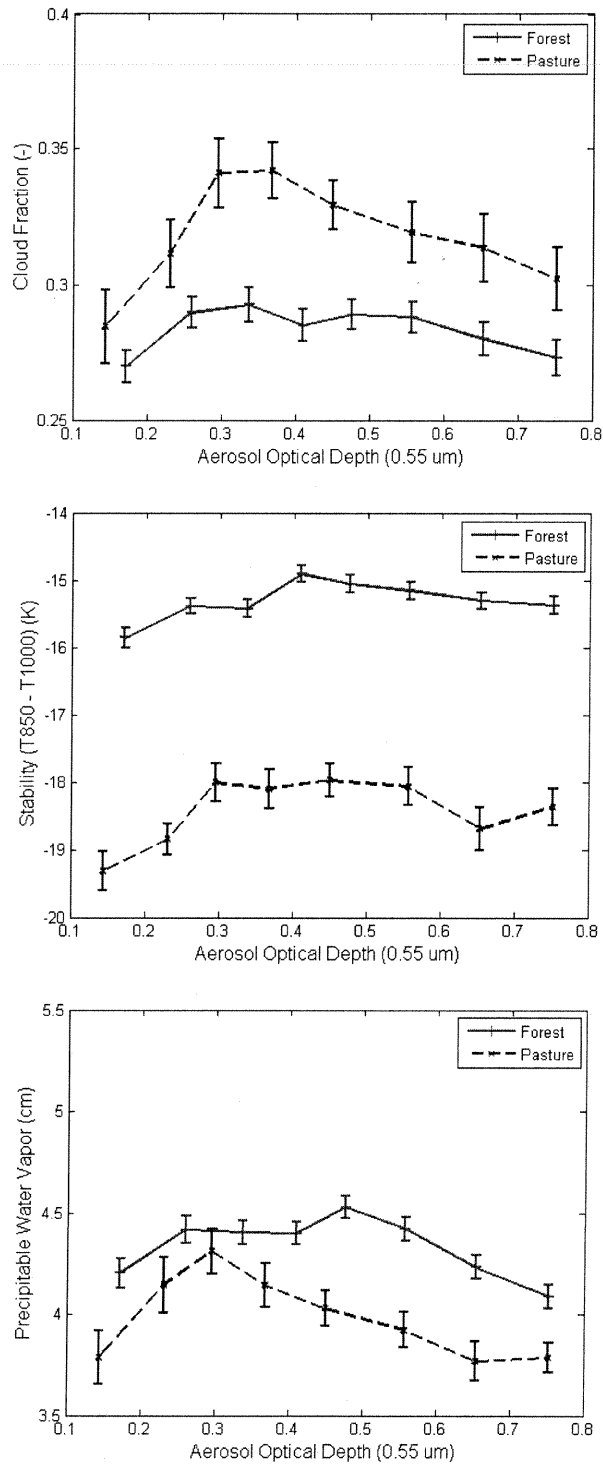


Figure 3(a): Cloud fraction binned by aerosol optical depth for all warm cloud retrievals with non-zero cloud fractions less than 0.5 for the months of August to October, for the years 2004, 2005, and 2007. **(b)** Atmospheric stability binned by aerosol optical depth, stratified by non-zero cloud fractions less than 0.5 for the time periods in (a). Stability is defined as the difference in temperature at 850 hPa and 1000 hPa. **(c)** Precipitable water binned by aerosol optical depth, stratified by non-zero cloud fractions less than 0.5 for the time periods in (a).

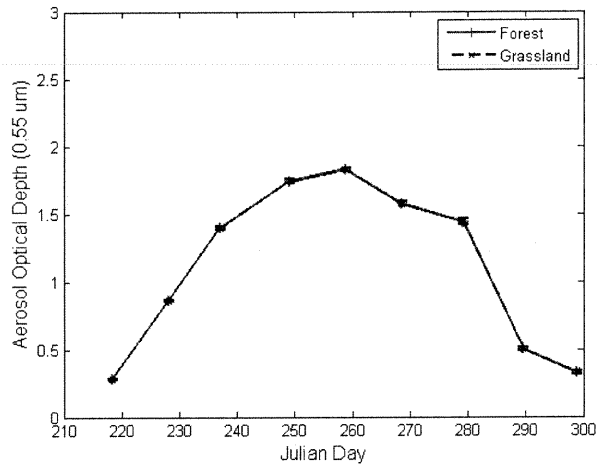


Figure 4: Aerosol optical depth binned by Julian Day for the years 2004, 2005, and 2007. The rate of increase of AOD with Julian Day is large in magnitude at the beginning of the season and at the end of the season.

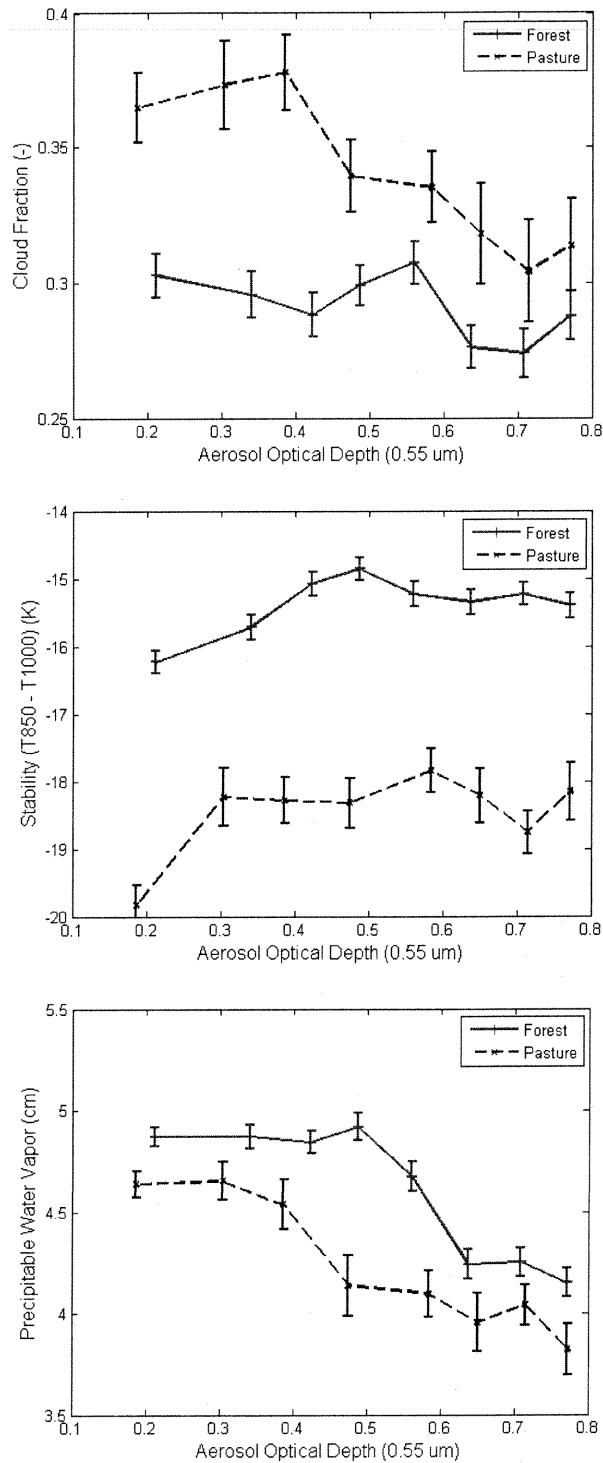


Figure 5(a): Cloud fraction binned by aerosol optical depth for all warm cloud retrievals with non-zero cloud fractions less than 0.5 for the days between August 15th and October 15th, for the years 2004, 2005, and 2007. **(b)** Atmospheric stability binned by aerosol optical depth, stratified by non-zero cloud fractions less than 0.5 for the time periods in (a). **(c)** Precipitable water binned by aerosol optical depth, stratified by non-zero cloud fractions less than 0.5 for the time periods in (a).

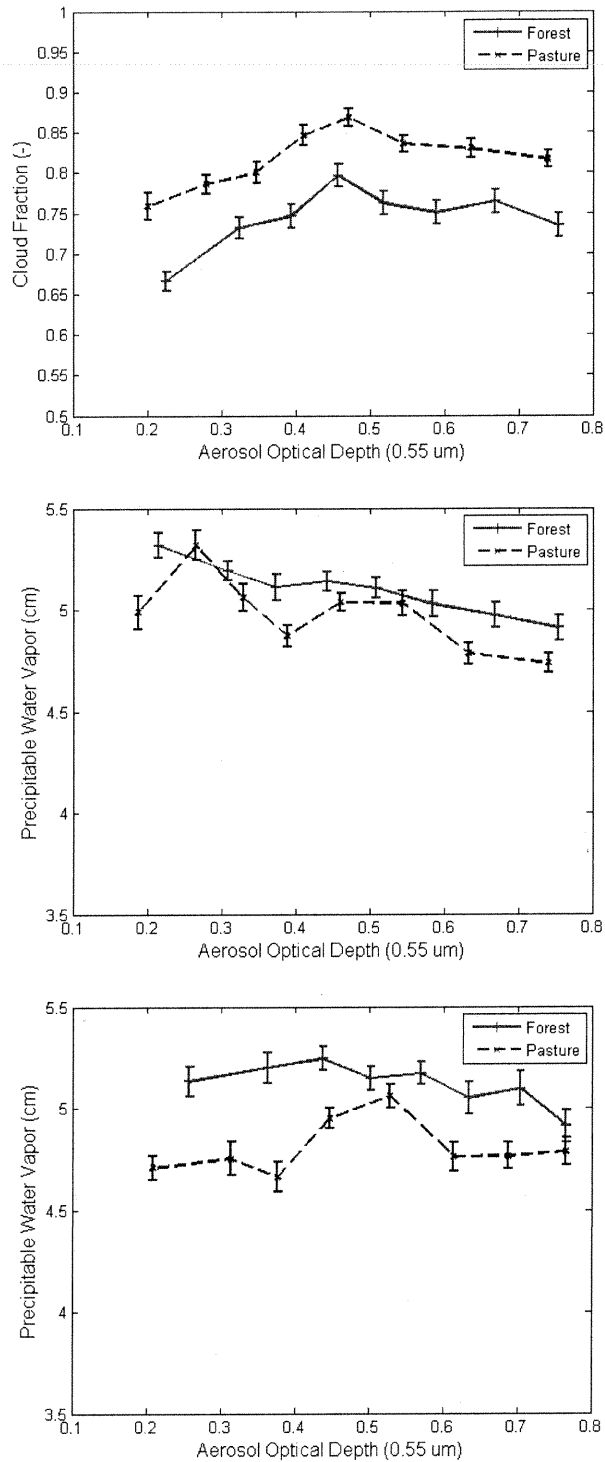


Figure 6(a): Cloud fraction binned by aerosol optical depth for all warm cloud retrievals with cloud fractions greater than 0.5 for the months of August to October, for the years 2004, 2005, and 2007. **(b)** Precipitable water binned by aerosol optical depth, stratified by cloud fractions greater than 0.5 for the time periods in (a). **(c)** Precipitable water binned by aerosol optical depth, stratified by cloud fractions greater than 0.5 for the days between August 15th and October 15th, for the years 2004, 2005, and 2007.

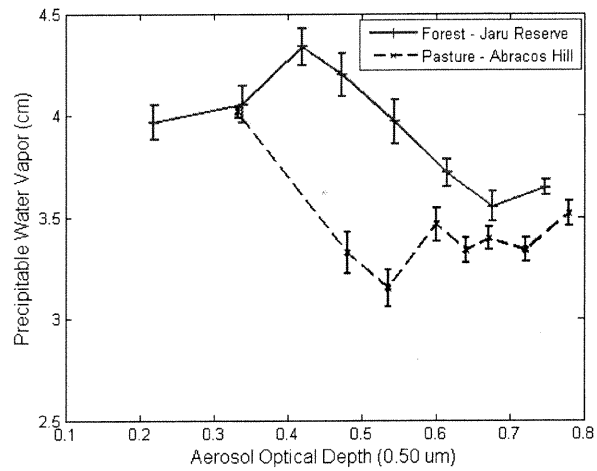
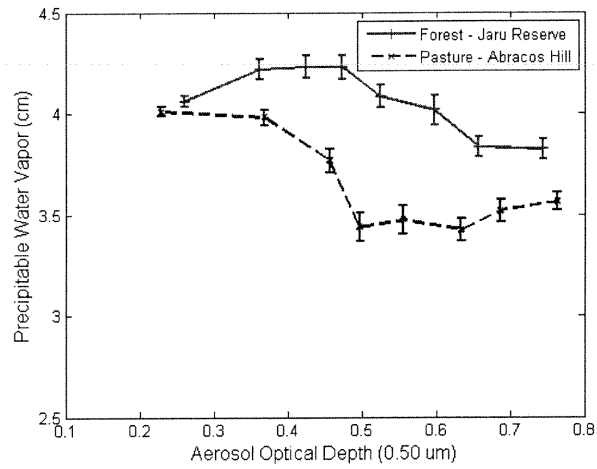


Figure 7(a): Precipitable water vapor binned by aerosol optical depth for two nearby AERONET stations, Jarú Reserve and Abracos Hill, for the time period between August 15th and October 15th, 2002. (b) Same as in (a) but for the time period between September 1st and September 30th, 2002.